



## Updated stock assessment of Pacific saury (*Cololabis saira*) in the Western North Pacific Ocean through 2021

Jhen Hsu<sup>1</sup>, Yi-Jay Chang<sup>1</sup>, Chih-hao Hsieh<sup>1</sup>, Wen-Bin Huang<sup>2</sup>, Tung-Hsieh Chiang<sup>3</sup>

1. Institute of Oceanography, National Taiwan University
2. Department of Natural Resources and Environmental Studies, National Dong Hwa University
3. Overseas Fisheries Development Council of Chinese Taipei

### Summary

This paper describes the updated stock assessment of the Pacific saury (*Cololabis saira*) in the Western North Pacific Ocean (WNPO) based on the guideline of the 2021 NPFC SSC PS07. The assessment consisted of applying the Bayesian state-space surplus production model for estimating the biomass from 1980 to 2021 with available catches from 1980 to 2020. Abundance indices available for WNPO Pacific saury consisted of standardized catch-per-unit-effort (CPUE) of stick-held dip net fisheries from Japan (1980 – 2020), Chinese Taipei (2001 – 2020), Russia (1994 – 2020), Korea (2001 – 2020), and China (2013 – 2020), and biomass survey from Japan (2003 – 2021). Two base case models were considered for the assessment outputs. The results of two base case models indicated that the estimated biomass trends before 2000 were sensitive to the early Japanese CPUE index (1980 – 1993). The ensemble time-series of biomass is estimated to have an increasing pattern since 2000 with the peaks in 2003, 2005 and 2008, after then dramatically decreased overtime and below  $B_{MSY}$  in 2015 – 2021. It should be noted that the models estimate the lowest biomass level in 2020 (median  $B_{2020}/B_{MSY} = 0.43$ , 80 percentile range 0.27 – 0.66) and following a slightly increase in 2021 (median  $B_{2021}/B_{MSY} = 0.55$ , 80 percentile range 0.35 – 0.85). An increasing trend in the fishing mortality is estimated from 2004 to 2018 and the recent average fishing mortality is estimated to be below  $F_{MSY}$  (median  $F_{2018-2020}/F_{MSY} = 0.94$ , 80 percentile range 0.48 – 1.90). It should be noted that the models estimate a slightly decreasing in the fishing mortality in 2020 (median  $F_{2020}/F_{MSY} = 0.75$ , 80 percentile range 0.40 – 1.42). The ensemble MCMC results from the two base cases indicated that the 2020 stock status is likely within the yellow quadrant (Prob [ $B_{2020} < B_{MSY}$  and  $F_{2020} < F_{MSY}$ ] = 71.56%).

### 1. Introduction

Here, we present an updated stock assessment of Pacific saury in the Western North Pacific Ocean (WNPO) of the North Pacific Fisheries Commission (NPFC) convention area. The assessment consisted of applying the Bayesian state-space surplus production model with available catches and standardized catch-per-unit-effort (CPUE) indices from the members from 1980 to 2020 and the Japanese biomass index from 2003 – 2021. The Bayesian method provided the direct estimates of uncertainty of the model parameters and management quantities. The objectives of this study are to conduct a stock assessment for the Pacific saury in the WNPO through 2020, to examine the sensitivity of the results to changes in model structural uncertainty, to determine the ensemble stock condition

from the developed base cases. Since the SSC PS agreed to not conduct the stock projections due to the poor predictive ability of the current Bayesian surplus production model (NPFC-2020-SSC PS06-Final Report), therefore we did not include the stock projection and its risk analysis in this updated stock assessment report.

## 2. Material and methods

Fishery catch data from 1950 – 2020 for assessing WNPO saury were taken from the most recent summary of available fishery-dependent data (NPFC-2021-SSC PS07-Final Report). The commercial catch of Pacific saury caught by Japan, Chinese Taipei, Korea, China, Russia and other members in the WNPO area were collected from 1950 to 2020 (**Figure 1**). Estimates of standardized fishery-dependent catch-per-unit-effort (CPUE) of WNPO Pacific saury were available for Japanese offshore stick-held dip net fisheries, however, Japanese standardized CPUE data was separated into two time series, one before 1994 (1980 – 1993) (NPFC-TWG PSSA03-WP11) and one from 1994 to 2020 (NPFC-2021-SSC-PS07-WP07) to account for the potential change in catchability. Indices of Chinese Taipei and Korean distant-water stick-held dip net fisheries were available from 2001 – 2020 (NPFC-2021-SSC PS07-WP14 and NPFC-2021-SSC PS07-WP18). Russia provided the abundance index of offshore and distant stick-held dip net fisheries from 1994 – 2020 (NPFC-2021-SSC PS07-WP02). Index of Chinese distant-water stick-held dip net fisheries was also available from 2013–2020 (NPFC-2021-SSC PS07-WP13) (**Figure 2a**). Fishery-independent biomass index was available from Japanese scientific research surveys from 2003 – 2021 by using mid-water trawl (NPFC-2021-SSC PS07-WP06) and the joint CPUE index (NPFC-2021-SSC PS07-WP16) was available from 2001–2020 (**Figure 2b**). Based on the SSC PS07 recommended base case scenarios (NPFC-2021-SSC PS07-Final Report), two base case models differed in the inclusion of the early Japanese CPUE and the observation error variance of the CPUEs were explored (**Table 1**). We also developed two sensitivity cases (**Table 1**) to evaluate the model outputs of the base cases following the recommendation of the SSC PS07 (NPFC-2021-SSC PS07-Final Report). The Bayesian analysis requires prior probability distributions for each of the model parameters. These priors were summarized in **Table 2**.

## 3. Results

### 3.1 Convergence of base case model

The visual inspection of trace plots of the major parameters showed the good mixing of the three chains (i.e., moving around the parameter space), also indicative of convergence of the MCMC chains. The Gelman and Rubin statistic for all parameters, including all variance terms, equalled 1, which indicated convergence of the Markov chains. Similarly, the Heidelberger and Welch test could not reject the hypothesis that the MCMC chains were stationary at the 95% confidence level for any of the parameters. Overall, these diagnostics indicated that the posterior distributions of the model parameters were adequately sampled with the MCMC simulations.

### 3.2 Model fits to catch-per-unit-effort indices

Plots of residual diagnostics by fishery for the base case models were shown in **Figures 3 – 4**. Models fit to the Chinese Taipei index had a residual trend with negative residuals in 2002 – 2010 and positive residuals in 2011 – 2020. Overall, the model fits to the WNPO Pacific saury indices indicated that there was a lack of fit to the Chinese Taipei CPUE.

### 3.3 Posterior estimates of model parameters

Plots of posterior densities of the parameters  $r$  (intrinsic growth rate),  $K$  (carrying capacity),  $M$  (shape parameter),  $\sigma^2$  (observation error),  $\tau^2$  (process error),  $b$  (Hyper-depletion/stability), and  $P_I$  (biomass depletion in 1980) for each base case were shown in **Figures 5 – 6**, together with their respective prior densities. Similar to the log-normal priors, the marginal posteriors generally have a long right-hand tail in the density plot. Summaries of parameters estimates of each of the base cases and their joint results were provided in **Tables S1 – S3**. The results of time-varying catchability ( $q$ ) in early Japanese CPUE (1980 – 1993) were shown in **Figure 7 and Table S1**.

### 3.4 Stock assessment results

Time-series of biomass ( $B$ ), the ratio of biomass to  $B_{MSY}$  ( $B/B_{MSY}$ ) and the biomass depletion ( $B/K$ ) within each base case and sensitivity case were provided in **Figures 8 – 9** and **Figures S1 – S4**, respectively. Different trends in biomass during 1980 – 1987 were found between base case 1 and base case 2 (**Figure 8**). However, the biomass trends after 2000 were consistent between the two base cases. The ensemble time-series of biomass is estimated to have an increasing pattern since 2000 with the peaks in 2003, 2005 and 2008, after then decreased overtime and below  $B_{MSY}$  in 2008 – 2021. It should be noted that the models estimate the lowest biomass level in 2020 (median  $B_{2020}/B_{MSY} = 0.43$ , 80 percentile range 0.27 – 0.66) and following a slightly increase in 2021 (median  $B_{2021}/B_{MSY} = 0.55$ , 80 percentile range 0.35 – 0.85) (**Figure 8 and Table 3**).

Time-series of the fishing mortality ( $F$ ) and the ratio of fishing mortality to ( $F/F_{MSY}$ ) within two base cases and two sensitivity cases were provided in **Figures 10 – 11** and **Figures S5 – S8**, respectively. Differences in trends for the ratio of fishing mortality during 1980 – 1993 were found between base cases 1 and 2. Since 1994, there were similar trends among the two base case models. The ensemble time-series of fishing mortality ratio trend from two base cases were shown in **Figure 10**. An increasing trend in the fishing mortality is estimated from 2004 to 2018 and the recent average fishing mortality is estimated to be below  $F_{MSY}$  (median  $F_{2018-2020}/F_{MSY} = 0.94$ , 80 percentile range 0.48 – 1.9). It should be noted that the models estimate a slightly decreasing in the fishing mortality in 2020 (median  $F_{2020}/F_{MSY} = 0.75$ , 80 percentile range 0.40 – 1.42).

The quantities of management interest reference points from joint estimates of the base cases 1 and 2 were shown in **Table 3**, and each of the base cases was shown in **Tables S4 and S5**, respectively. Overall, the ensemble MCMC results from the two base cases indicated that the 2020 stock status is likely within the yellow quadrant (Prob [ $B_{2020} < B_{MSY}$  and  $F_{2020} < F_{MSY}$ ] = 71.56%) (**Figure 12**).

In addition, the Kobe plots in last year and the recent three years were also shown in **Figures S9 – S10**. The ensemble MCMC results from two base cases also suggested that the stock status of Pacific saury is located at the yellow quadrant.

### 3.5 Retrospective analysis

Retrospective analyses show that the time-series of  $B/B_{MSY}$  and  $F/F_{MSY}$  estimated by each of the base cases with the removal of the most 6 years of data (catch: 2016 – 2020; Japan biomass survey: 2016 – 2021) in successive model runs generally match well with the full-time series assessment (**Figures 13 – 14**). This suggested that there is generally no consistent pattern of bias in the estimates of  $B/B_{MSY}$  and  $F/F_{MSY}$ .

Table 1. Specifications of the two base case models and two sensitivity case models. “JPN\_early” = early Japan (1980 – 1993), “JPN\_late” = late Japan (1994 – 2020), “CT” = Chinese Taipei, “RUS” = Russia, “KOR” = Korea, “CHN” = China, “JPN\_bio” = Japan biomass survey.  $q_1$  = fishing efficiency of the Japanese mid-water trawl net;  $q$  = generic catchability of the Japanese biomass survey.

	Base case1	Base case2	Sensitivity case1	Sensitivity case2
Initial year		1980		
Biomass survey		$B_{obs} = B_{est} \times q_1 \sim \text{LN}(\log(q \times B), s^2)$		
		$q \sim U(0,1)$		
CPUE index	CHN (2013-2020) JPN_early (1980-1993) (time-varying $q$ ) JPN_late (1994-2020) KOR (2001-2020) RUS (1994-2020) CT (2001-2020) $I_{i,f} = q_f B_i^b e^{v_{i,f}}$ $v_{i,f} \sim N(0, \sigma_f^2)$ $\sigma_f^2 = c \times (\text{ave}(CV_i^2) + \sigma_{bio}^2)$ where $\text{ave}(CV_i^2)$ is computed except for 2020 biomass survey	CHN (2013-2020) JPN_late (1994-2020) KOR (2001-2020) RUS (1994-2020) CT (2001-2020) $I_{i,f} = q_f B_i^b e^{v_{i,f}}$ $v_{i,f} \sim N(0, \sigma_f^2)$ $\sigma_f^2 = c \times (\text{ave}(CV_i^2) + \sigma_{bio}^2)$ where $\text{ave}(CV_i^2)$ is computed except for 2020 biomass survey	JPN_early (1980-1993) (time-varying $q$ ) Joint CPUE (2001-2020)	Joint CPUE (2001-2020)
Variance component	Variance of logCPUEs are assumed to be common and 6 times of that of log biomass ( $c = 6$ )	Variance of logCPUEs are assumed to be common and 5 times of that of log biomass ( $c = 5$ )	Same weight between biomass and joint CPUE	
Hyper-depletion/stability	$b \sim U(0,1)$ but [b_JPN_early=1]	$b \sim U(0,1)$	$b \sim U(0,1)$	$b \sim U(0,1)$

Table 2. Summary of the specified priors for the Bayesian state-space models. “JPN1” = early Japan (1980 – 1993), “JPN2” = late Japan (1994 – 2020), “CT” = Chinese Taipei, “RUS” = Russia, “KOR” = Korea, “CHN” = China, “JPN\_bio” = Japan biomass survey.

Parameter	Description	Prior
$K$	Carrying capacity (10,000 mt)	$K \sim \log N\left(\log(150) - \frac{\sigma_K^2}{2}, \sigma_K^2\right); CV_K = 1$
$r$	Intrinsic growth rate (year <sup>-1</sup> )	$r \sim \log N\left(\log(1.4) - \frac{\sigma_r^2}{2}, \sigma_r^2\right); CV_r = 2$
$M$	Shape parameter	$M \sim \text{Gamma}(2,2)$
$q$	Catchability for others fleets (JPN2;CT; RUS; KOR and CHN)	$1/q \sim \text{Gamma}(0.01,0.01)$
$q_{bio}$	Catchability for Japanese survey biomass	$q_{bio} \sim \text{Uniform}(0,1)$
$q_{JPN1}^{1980}$	Time-varying catchability for JPN1 in 1980	$q_{JPN1}^{1980} \sim \text{Uniform}(1 \times 10^{-7}, 2)$
$\omega$	Annual deviations of the log-scale time-varying catchability	$\omega \sim N(0, 0.1)$
$\beta$	Hyperstability of 1994-2019	$\beta \sim \text{Uniform}(0,1)$
$\sigma^2$	Common observation error of CPUE	$1/\sigma^2 \sim \text{Gamma}(2,0.45); CV_\tau = 1$
$\tau^2$	Process error	$1/\tau^2 \sim \text{Gamma}(4,0.1)$
$P_1$	Initial condition ( $B_1/K$ )	$P_1 \sim \log N\left(\log(0.7) - \frac{\sigma_{R_1}^2}{2}, \sigma_{R_1}^2\right); CV_{R_1} = 1$

$$CV_\theta = \left(\exp(\sigma_\theta^2) - 1\right)^{1/2}$$

Table 3. Summary of joint estimates of reference points of the base cases 1 and 2.

	Mean	Median	Lower 10th	Upper 10th
Catch <sub>2020</sub>	13.97	13.97	13.97	13.97
F <sub>2018-2020</sub>	0.59	0.36	0.15	0.99
F <sub>2020</sub>	0.43	0.29	0.13	0.75
F <sub>M<sub>SY</sub></sub>	0.46	0.41	0.21	0.75
MSY	43.65	42.14	32.69	56.18
F <sub>2020</sub> /F <sub>M<sub>SY</sub></sub>	0.88	0.75	0.4	1.42
F <sub>2018-2020</sub> /F <sub>M<sub>SY</sub></sub>	1.15	0.94	0.48	1.9
K	296	268.4	166.6	463.3
B <sub>2020</sub>	65.61	55.2	26.38	117.67
B <sub>2021</sub>	83.76	70.37	34.81	149.2
B <sub>2019-2021</sub>	80.37	67.94	33.56	143.16
B <sub>M<sub>SY</sub></sub>	141.41	127.7	79.98	220.2
B <sub>M<sub>SY</sub></sub> /K	0.52	0.47	0.29	0.79
B <sub>2020</sub> /K	0.21	0.21	0.13	0.3
B <sub>2021</sub> /K	0.27	0.27	0.17	0.39
B <sub>2019-2021</sub> /K	0.26	0.26	0.17	0.36
B <sub>2020</sub> /B <sub>M<sub>SY</sub></sub>	0.45	0.43	0.27	0.66
B <sub>2021</sub> /B <sub>M<sub>SY</sub></sub>	0.58	0.55	0.35	0.85
B <sub>2019-2021</sub> /B <sub>M<sub>SY</sub></sub>	0.55	0.53	0.35	0.79

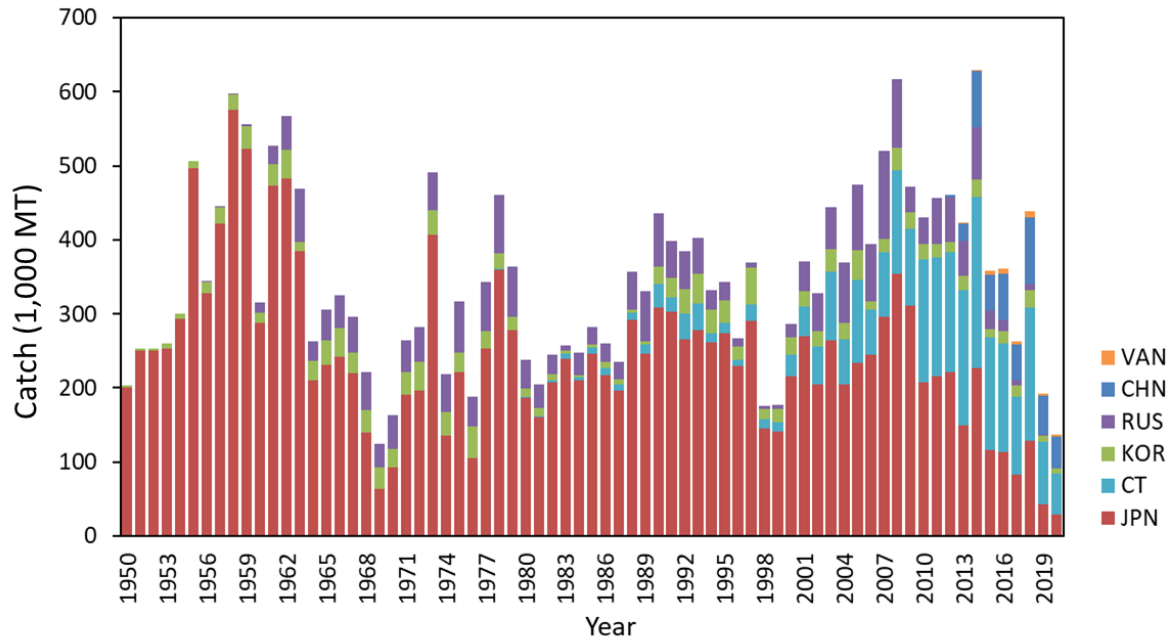


Figure 1. Time-series of catches (metric ton) of the Pacific saury in the Western North Pacific Ocean from 1950 to 2020 by the members.

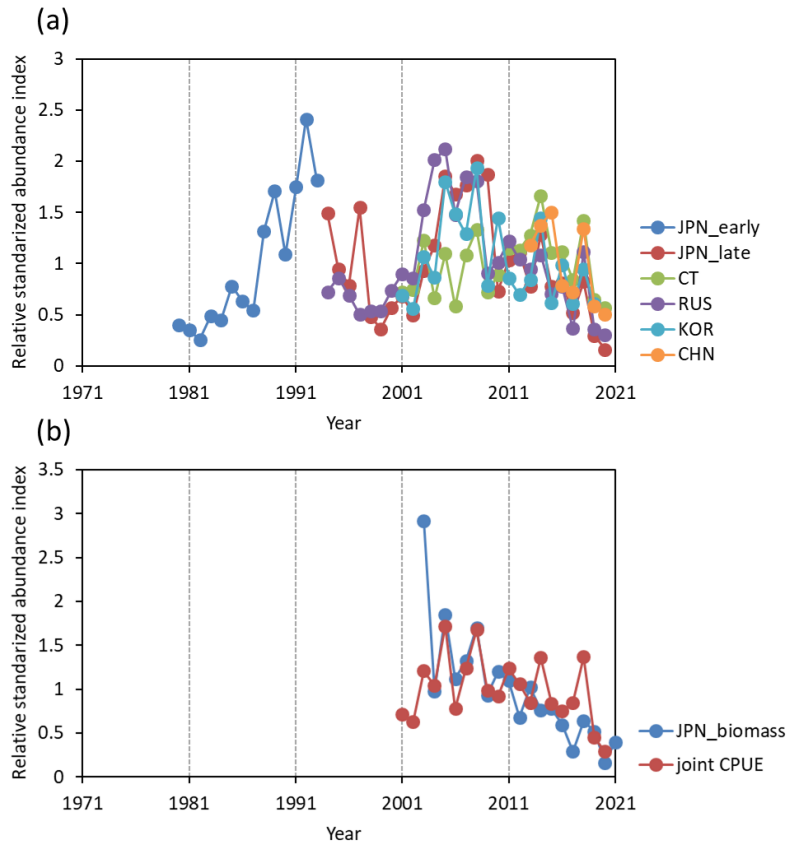


Figure 2. Pacific saury CPUE indices (a) from early Japan (JPN\_early), late Japan (JPN\_late), Chinese Taipei (CT), Russia (RUS), Korea (KOR), and China (CHN) stick-held dip net fisheries during 1980 - 2020, and (b) biomass survey index of Japan (JPN\_biomass) and joint CPUE index during 2001 - 2021 in the Western North Pacific Ocean.

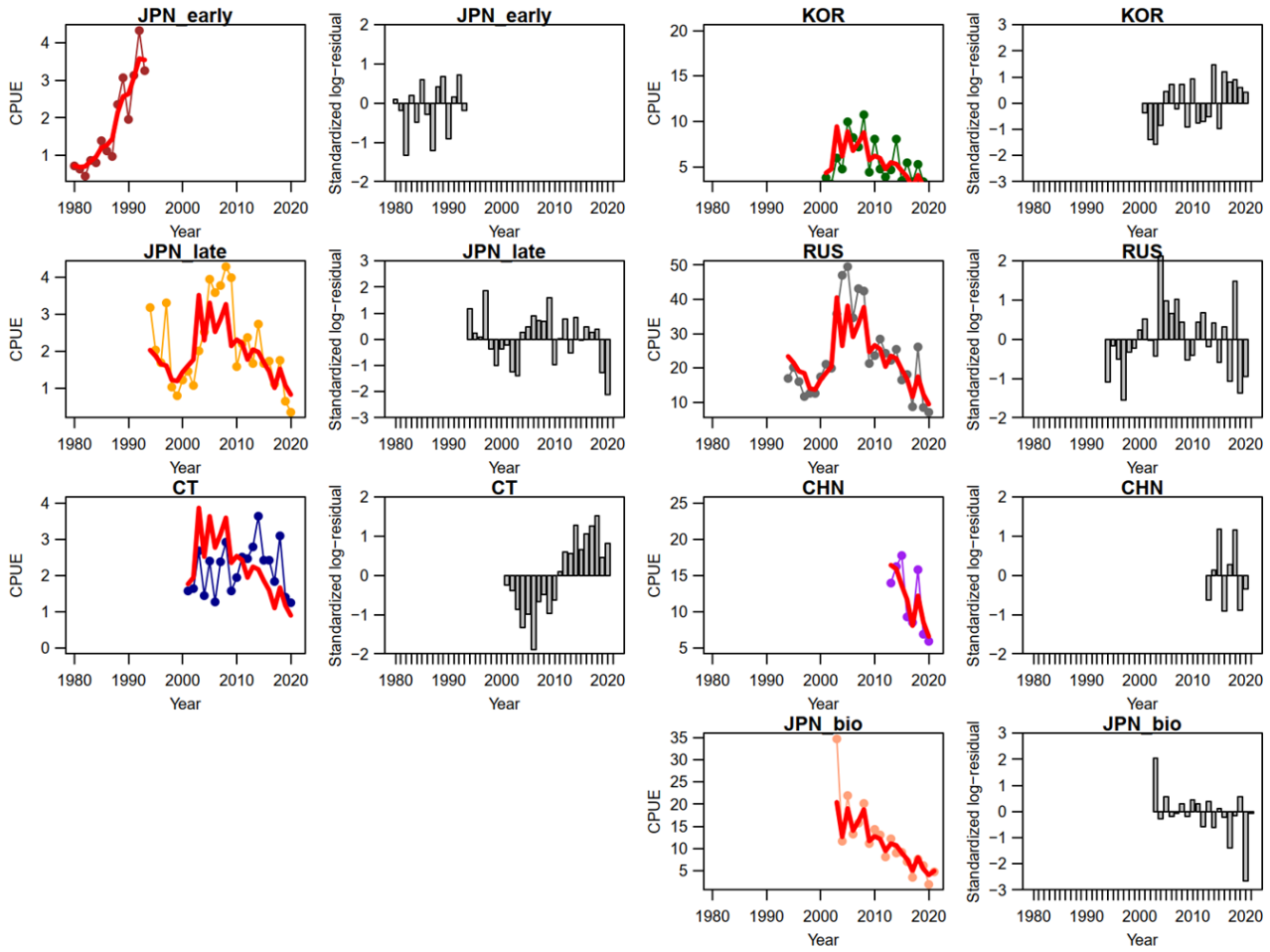


Figure 3. Time-series of observed (circle-line) and predicted (red solid line) catch per unit effort (CPUE) of Western North Pacific saury and standardized log-residuals for the base case 1 production model. “JPN\_early” = early Japan (1980-1993), “JPN\_late”=late Japan (1994-2020), “CT” = Chinese Taipei, “RUS” = Russia, “KOR”= Korea, “CHN”=China, JPN\_bio” = Japanese biomass survey.

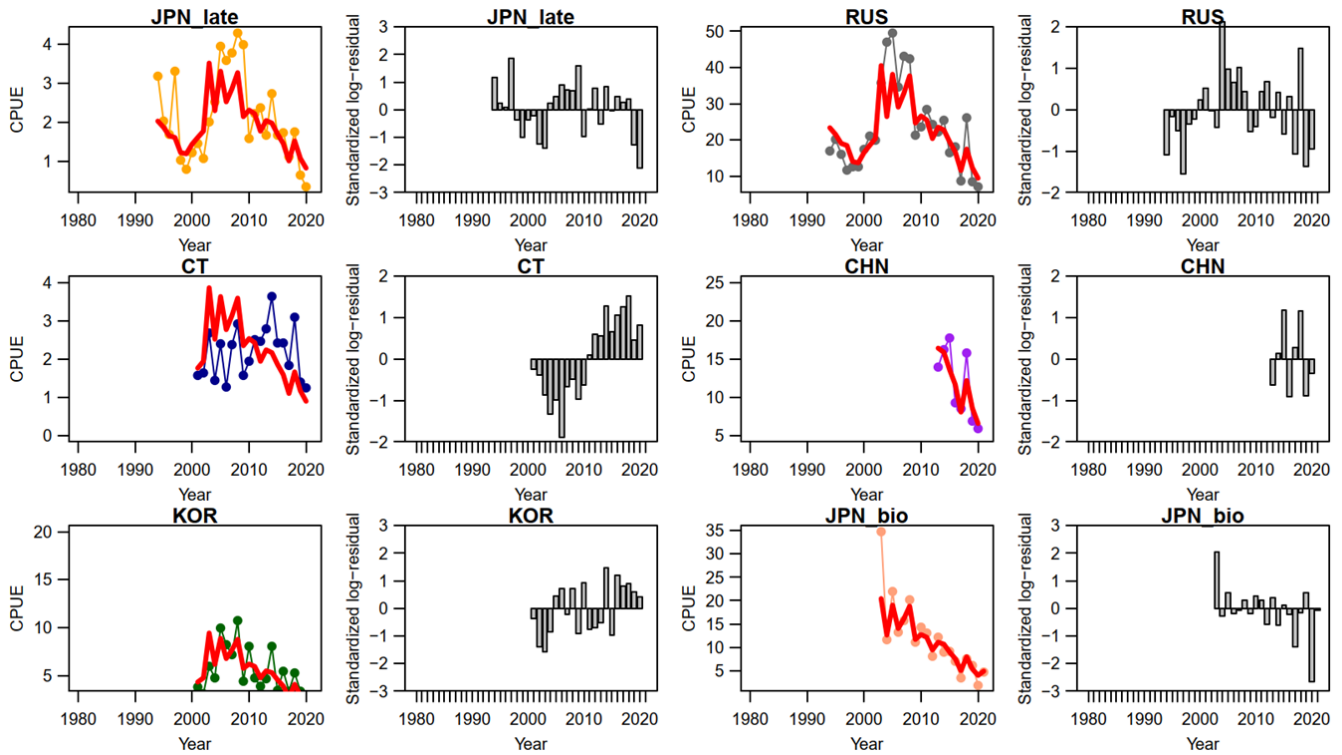


Figure 4. Time-series of observed (circle-line) and predicted (red solid line) catch per unit effort (CPUE) of Western North Pacific saury and standardized log-residuals for the base case 2 production model. “JPN\_late”=late Japan (1994-2020), “CT” = Chinese Taipei, “RUS” = Russia, “KOR”= Korea, “CHN”=China, “JPN\_bio” = Japanese biomass survey.

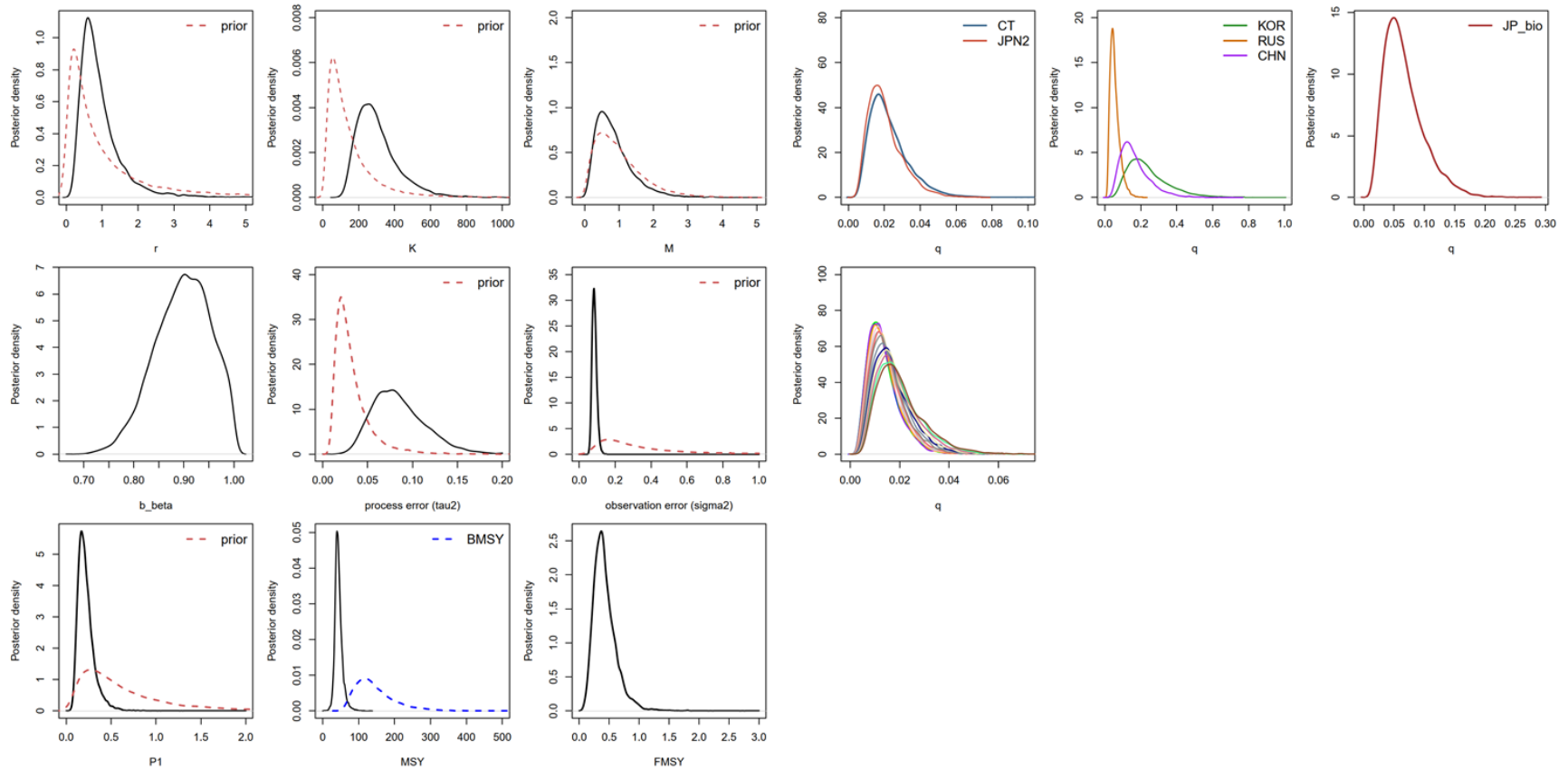


Figure 5. Kernel density estimates of the posterior distributions (solid lines) of various model parameters and management quantities for the base case 1 production model for the Pacific saury in the Western North Pacific Ocean. Proper prior densities are given by the dashed lines. “JPN2”=late Japan (1994-2020), “CT” = Chinese Taipei, “RUS” = Russia, “KOR”= Korea, “CHN”=China, “JP\_bio” = Japanese biomass survey.

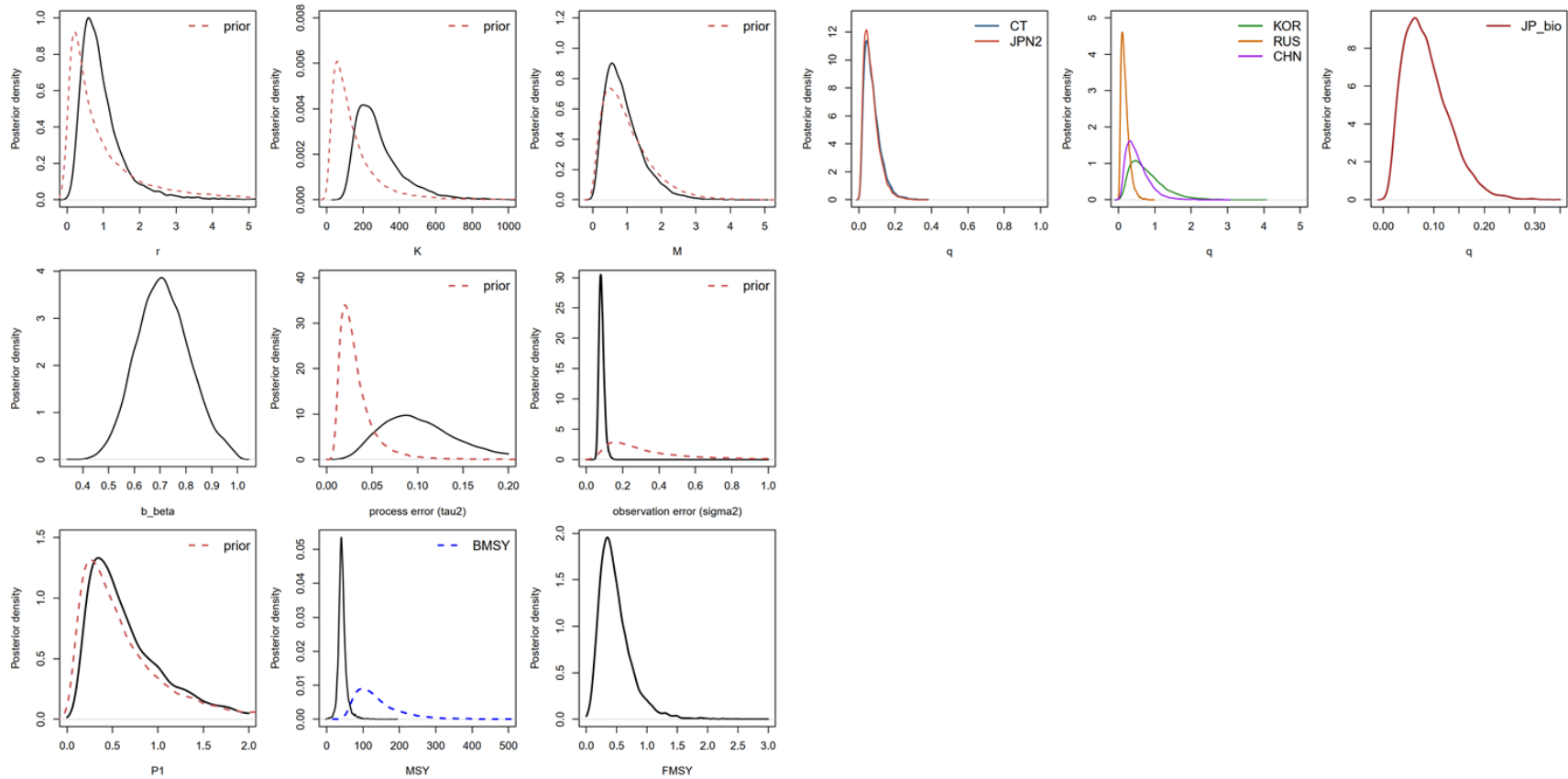


Figure 6. Kernel density estimates of the posterior distributions (solid lines) of various model parameters and management quantities for the base case 2 production model for the Pacific saury in the Western North Pacific Ocean. Proper prior densities are given by the dashed lines. “JPN2”=late Japan (1994-2020), “CT” = Chinese Taipei, “RUS” = Russia, “KOR”= Korea, “CHN”=China, “JP\_bio” = Japanese biomass survey.

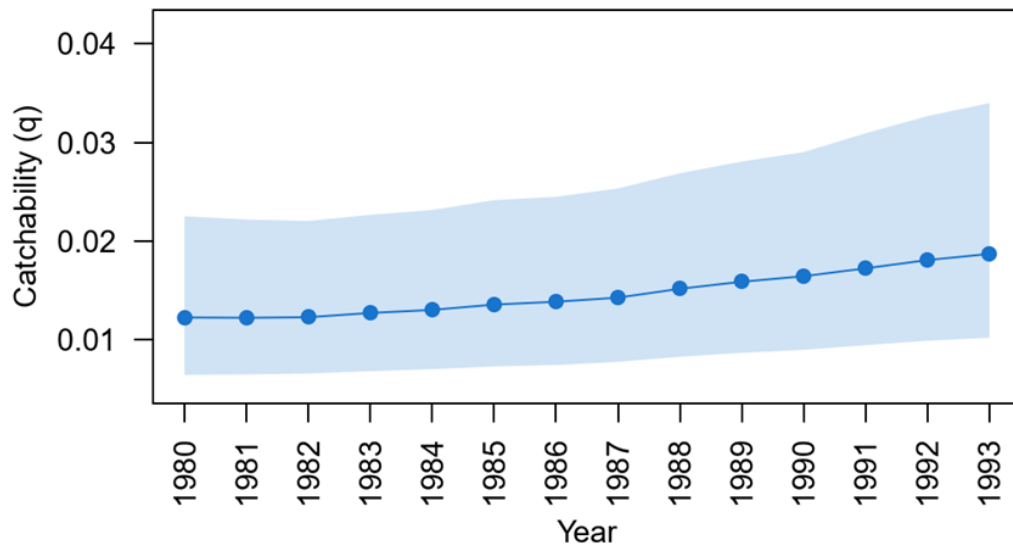


Figure 7. Time series estimates of annual catchabilities of the early Japanese CPUE from 1980 to 1993 for the base case 1.

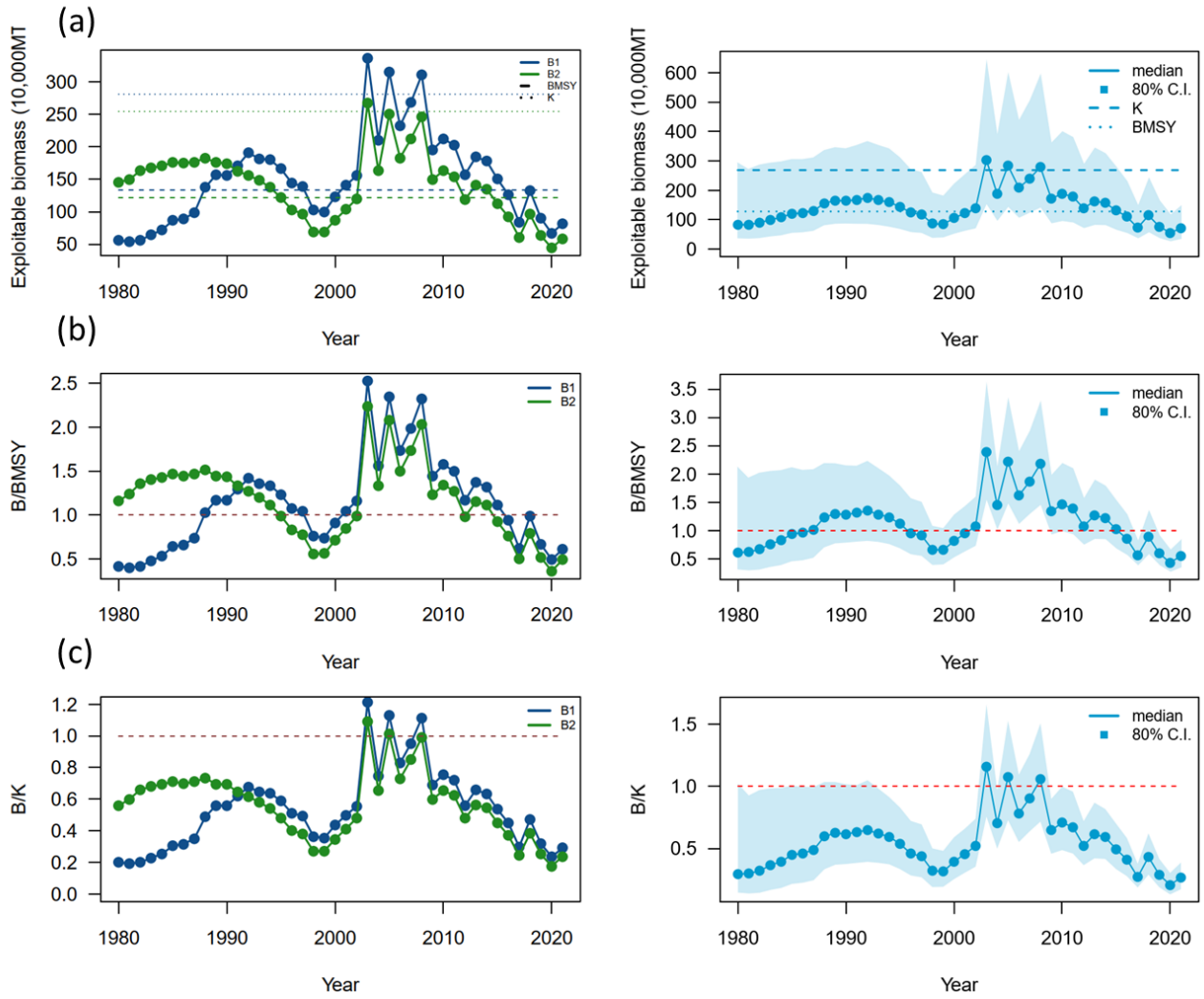


Figure 8. Time series of ensemble biomass (10,000 metric ton) (a), the ratio of biomass to  $B_{MSY}$  ( $B/B_{MSY}$ ) (b), and the depletion ratio ( $B/K$ ) of the western North Pacific saury for the base case 1-2 (B1 and B2, respectively; left panel) and the median estimates of MCMC results from base cases 1-2 (right panel). In panel (a), the upper dashed and lower dotted horizontal line denotes the carrying capacity ( $K$ ) and  $B_{MSY}$ , respectively. In panels (b) and (c), the dashed lines denote the reference levels of 1.

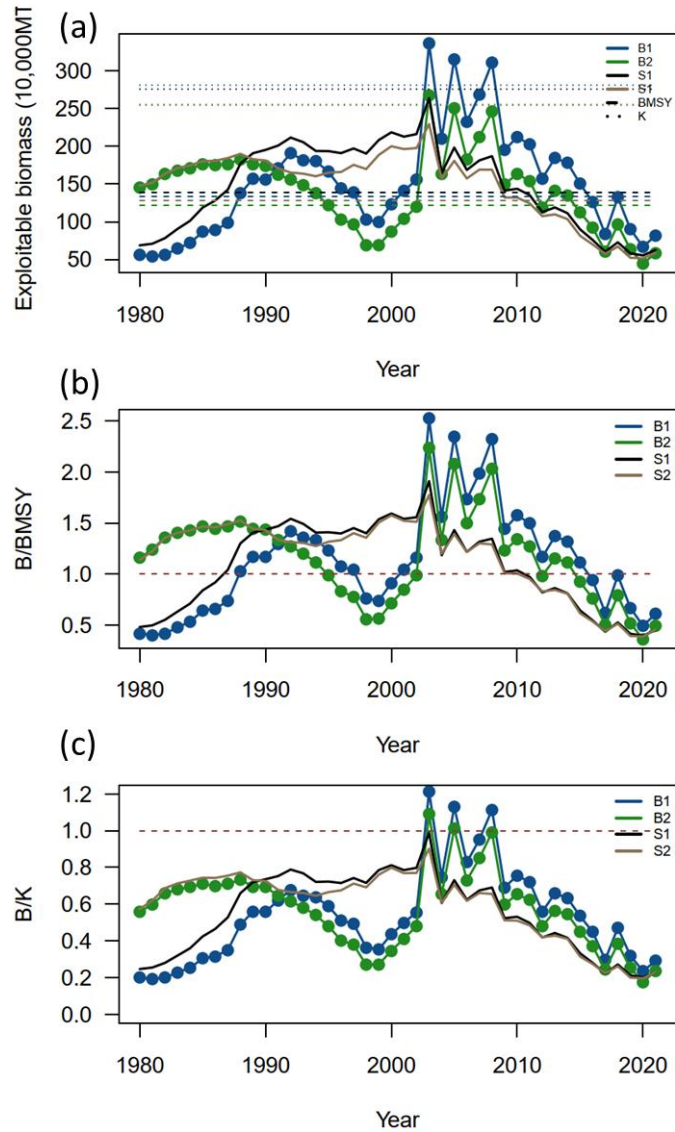


Figure 9. Time series of ensemble biomass (10,000 metric ton) (a), the ratio of biomass to  $B_{MSY}$  ( $B/B_{MSY}$ ) (b), and the depletion ratio ( $B/K$ ) (c) of the western North Pacific saury for the base case 1-2 (B1 and B2, respectively) and sensitivity cases 1-2 (S1 and S2, respectively). In panel (a), the upper dashed and lower dotted horizontal line denotes the carrying capacity ( $K$ ) and  $B_{MSY}$ , respectively. In panels (b) and (c), the dashed lines denote the reference levels of 1.

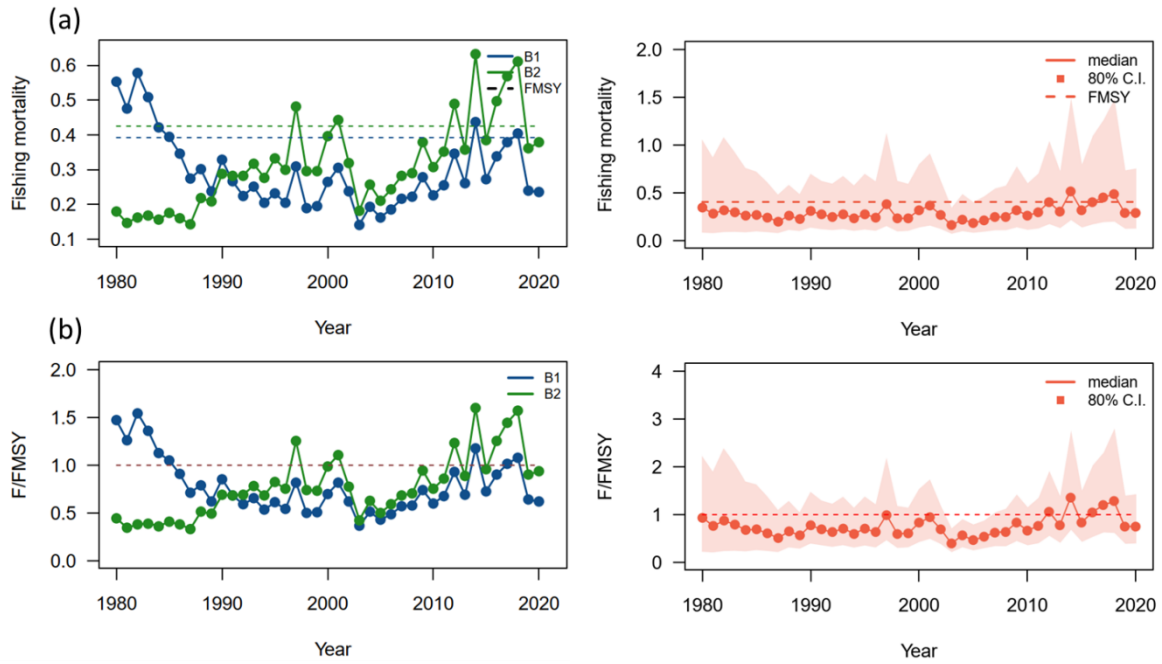


Figure 10. Time series of fishing mortality (a), and the ratio of fishing mortality to  $F_{MSY}$  ( $F/F_{MSY}$ ) (b) of the western North Pacific saury for the base case 1-2 (B1 and B2, respectively; left panel) and the median estimates of MCMC results from base cases 1-2 (right panel). In panel (a), the upper dashed and lower dotted horizontal line denotes the  $F_{MSY}$ , respectively. In panels (b), the dashed lines denote the reference levels of 1.

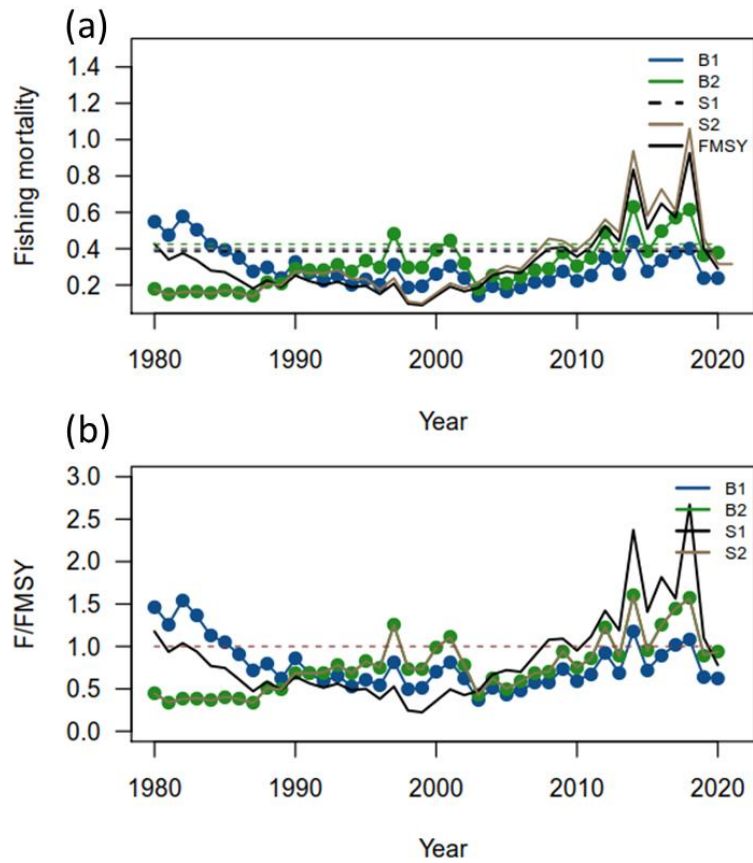


Figure 11. Time series of fishing mortality (a), and the ratio of fishing mortality to  $F_{MSY}$  ( $F/F_{MSY}$ ) (b) of the western North Pacific saury for the base case 1-2 (B1 and B2, respectively) and sensitivity case 1-2 (S1 and S2, respectively). In panel (a), the upper dashed and lower dotted horizontal line denotes the  $F_{MSY}$ , respectively. In panels (b), the dashed lines denote the reference levels of 1.

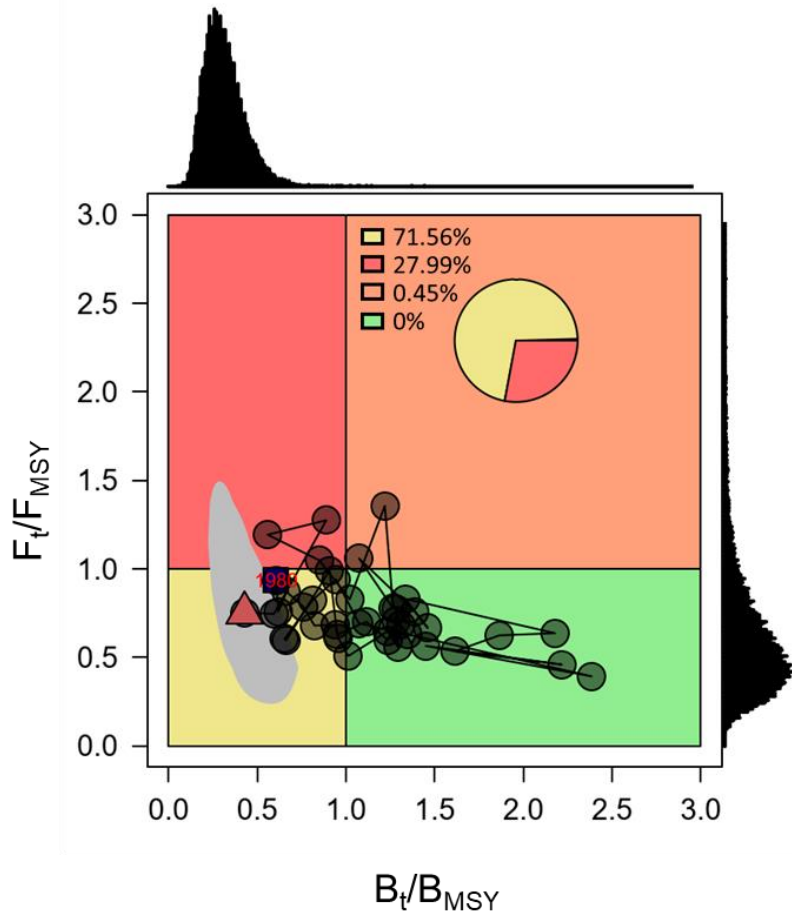


Figure 12. Ensemble Kobe phase plot of the stock trajectory of the western North Pacific saury from 1980 to 2020 (in red triangle) with uncertainty estimate in 2020 (80% credible intervals, grey polygon) from the two base case models.

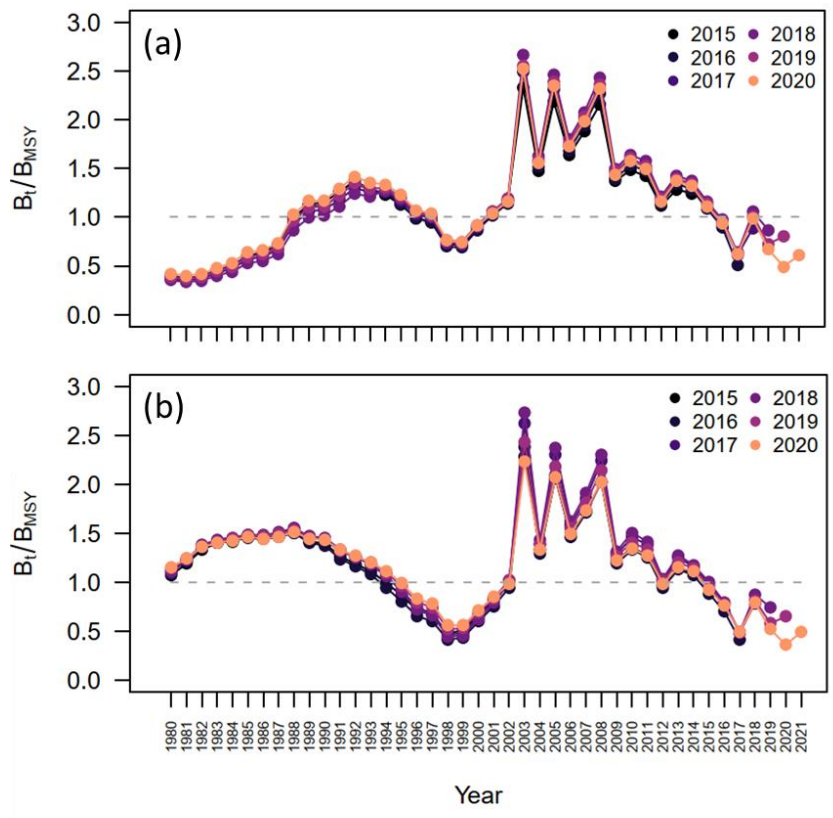


Figure 13. Six years within-model retrospective plots of the change in biomass to  $B_{MSY}$  of the western North Pacific saury from the base case 1 (a) and 2 (b).

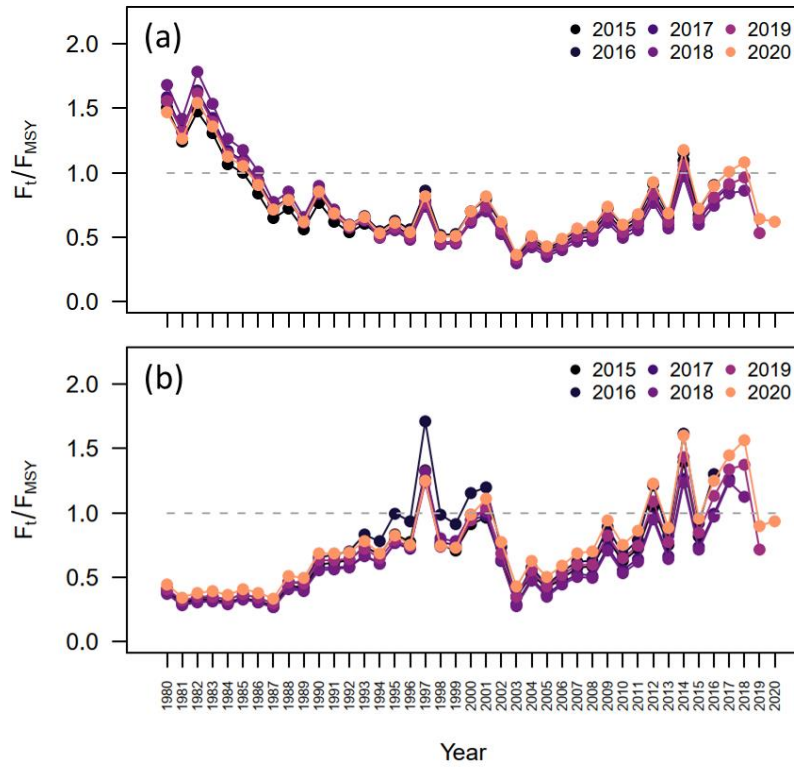


Figure 14. Six years within-model retrospective plots of the change in fishing mortality to  $F_{MSY}$  of the Western North Pacific saury from the base case 1 (a) and 2 (b).

## Supplementary

Table S1. Summary of parameter estimates of the base case 1.

	Mean	Median	Lower 10th	Upper 10th
$r$	0.96	0.79	0.41	1.65
$K$	304.74	281.25	179.61	461.70
$q_{CHN}$	0.17	0.15	0.08	0.28
$q_{JPN2}$	0.02	0.02	0.01	0.03
$q_{KOR}$	0.24	0.22	0.12	0.40
$q_{RUS}$	0.06	0.05	0.03	0.09
$q_{CT}$	0.02	0.02	0.01	0.04
$q_{Bio}$	0.07	0.06	0.03	0.11
Shape parameter ( $M$ )	0.85	0.73	0.30	1.57
observation error ( $\sigma_{com}$ )	0.29	0.29	0.26	0.32
observation error ( $\sigma_{bio}$ )	0.12	0.12	0.11	0.13
process error( $\tau$ )	0.29	0.29	0.22	0.36
$F_{MSY}$	0.43	0.39	0.22	0.67
$B_{MSY}$	144.98	132.95	85.58	219.80
$MSY$	44.18	42.65	33.39	56.72
$b$	0.90	0.90	0.82	0.97
$q_{JPN1\_1980}$	0.014	0.012	0.006	0.023
$q_{JPN1\_1981}$	0.014	0.012	0.006	0.022
$q_{JPN1\_1982}$	0.014	0.012	0.007	0.022
$q_{JPN1\_1983}$	0.014	0.013	0.007	0.023
$q_{JPN1\_1984}$	0.014	0.013	0.007	0.023
$q_{JPN1\_1985}$	0.015	0.014	0.007	0.024
$q_{JPN1\_1986}$	0.015	0.014	0.007	0.024
$q_{JPN1\_1987}$	0.016	0.014	0.008	0.025
$q_{JPN1\_1988}$	0.017	0.015	0.008	0.027
$q_{JPN1\_1989}$	0.017	0.016	0.009	0.028
$q_{JPN1\_1990}$	0.018	0.016	0.009	0.029
$q_{JPN1\_1991}$	0.019	0.017	0.009	0.031
$q_{JPN1\_1992}$	0.020	0.018	0.010	0.033
$q_{JPN1\_1993}$	0.021	0.019	0.010	0.034

Table S2. Summary of parameter estimates of the base case 2.

	Mean	Median	Lower 10th	Upper 10th
$r$	0.98	0.81	0.39	1.71
$K$	287.27	254.50	157.01	465.07
$q_{CHN}$	0.52	0.46	0.20	0.93
$q_{JPN2}$	0.07	0.06	0.03	0.13
$q_{KOR}$	0.79	0.69	0.30	1.43
$q_{RUS}$	0.18	0.16	0.07	0.33
$q_{CT}$	0.08	0.06	0.03	0.14
$q_{Bio}$	0.09	0.08	0.04	0.15
shape parameter ( $M$ )	0.90	0.79	0.32	1.65
observation error ( $\sigma_{com}$ )	0.29	0.29	0.26	0.32
observation error ( $\sigma_{bio}$ )	0.13	0.13	0.12	0.14
process error ( $\tau$ )	0.32	0.31	0.23	0.41
$F_{MSY}$	0.49	0.43	0.21	0.82
$B_{MSY}$	137.84	122.25	75.63	221.40
$MSY$	43.11	41.62	31.86	55.61
$b$	0.71	0.71	0.58	0.85

Table S3. Summary of joint estimates of parameters of the base cases 1 and 2.

	Mean	Median	Lower 10th	Upper 10th
<i>r</i>	0.97	0.80	0.40	1.67
<i>K</i>	296.01	268.40	166.60	463.30
<i>qCHN</i>	0.35	0.24	0.10	0.75
<i>qJPN2</i>	0.05	0.03	0.01	0.10
<i>qKOR</i>	0.52	0.35	0.14	1.13
<i>qRUS</i>	0.12	0.08	0.03	0.26
<i>qCT</i>	0.05	0.03	0.01	0.11
<i>qBio</i>	0.08	0.07	0.03	0.13
shape parameter ( <i>M</i> )	0.88	0.76	0.30	1.61
observation error ( $\sigma_{com}$ )	0.29	0.29	0.26	0.32
observation error ( $\sigma_{bio}$ )	0.12	0.12	0.11	0.14
process error ( $\tau$ )	0.30	0.30	0.23	0.39
$F_{MSY}$	0.46	0.41	0.21	0.75
$B_{MSY}$	141.41	127.70	79.97	220.20
$MSY$	43.65	42.14	32.69	56.19
<i>b</i>	0.81	0.83	0.62	0.95

Table S4. Summary of reference points of the base case 1.

	Mean	Median	Lower 10th	Upper 10th
Catch <sub>2020</sub>	13.97	13.97	13.97	13.97
F <sub>2018-2020</sub>	0.39	0.29	0.14	0.69
F <sub>2020</sub>	0.29	0.24	0.11	0.51
F <sub>MSY</sub>	0.43	0.39	0.22	0.67
MSY	44.18	42.65	33.39	56.72
F <sub>2020</sub> /F <sub>MSY</sub>	0.67	0.62	0.35	1.04
F <sub>2018-2020</sub> /F <sub>MSY</sub>	0.88	0.79	0.44	1.37
K	304.74	281.25	179.61	461.70
B <sub>2020</sub>	76.34	66.66	34.77	130.09
B <sub>2021</sub>	93.50	81.73	42.32	159.49
B <sub>2019-2021</sub>	91.18	79.88	42.12	154.76
B <sub>MSY</sub>	144.98	132.95	85.58	219.80
B <sub>MSY</sub> /K	0.48	0.47	0.42	0.55
B <sub>2020</sub> /K	0.24	0.24	0.17	0.33
B <sub>2021</sub> /K	0.30	0.29	0.20	0.41
B <sub>2019-2021</sub> /K	0.29	0.28	0.21	0.38
B <sub>2020</sub> /B <sub>MSY</sub>	0.52	0.49	0.34	0.72
B <sub>2021</sub> /B <sub>MSY</sub>	0.63	0.61	0.41	0.90
B <sub>2019-2021</sub> /B <sub>MSY</sub>	0.62	0.59	0.42	0.84

Table S5. Summary of reference points of the base case 2.

	Mean	Median	Lower 10th	Upper 10th
Catch <sub>2020</sub>	13.97	13.97	13.97	13.97
F <sub>2018-2020</sub>	0.78	0.46	0.17	1.32
F <sub>2020</sub>	0.58	0.38	0.15	0.96
F <sub>M<sub>SY</sub></sub>	0.49	0.43	0.21	0.82
MSY	43.11	41.62	31.86	55.61
F <sub>2020</sub> /F <sub>M<sub>SY</sub></sub>	1.10	0.94	0.49	1.71
F <sub>2018-2020</sub> /F <sub>M<sub>SY</sub></sub>	1.42	1.16	0.57	2.34
K	287.27	254.50	157.01	465.07
B <sub>2020</sub>	54.88	44.33	22.68	99.79
B <sub>2021</sub>	74.02	58.76	30.59	135.89
B <sub>2019-2021</sub>	69.57	55.68	29.10	127.17
B <sub>M<sub>SY</sub></sub>	137.84	122.25	75.63	221.40
B <sub>M<sub>SY</sub></sub> /K	0.48	0.48	0.42	0.55
B <sub>2020</sub> /K	0.18	0.18	0.12	0.26
B <sub>2021</sub> /K	0.25	0.24	0.16	0.36
B <sub>2019-2021</sub> /K	0.23	0.23	0.15	0.32
B <sub>2020</sub> /B <sub>M<sub>SY</sub></sub>	0.39	0.36	0.24	0.56
B <sub>2021</sub> /B <sub>M<sub>SY</sub></sub>	0.52	0.49	0.32	0.77
B <sub>2019-2021</sub> /B <sub>M<sub>SY</sub></sub>	0.49	0.46	0.31	0.70

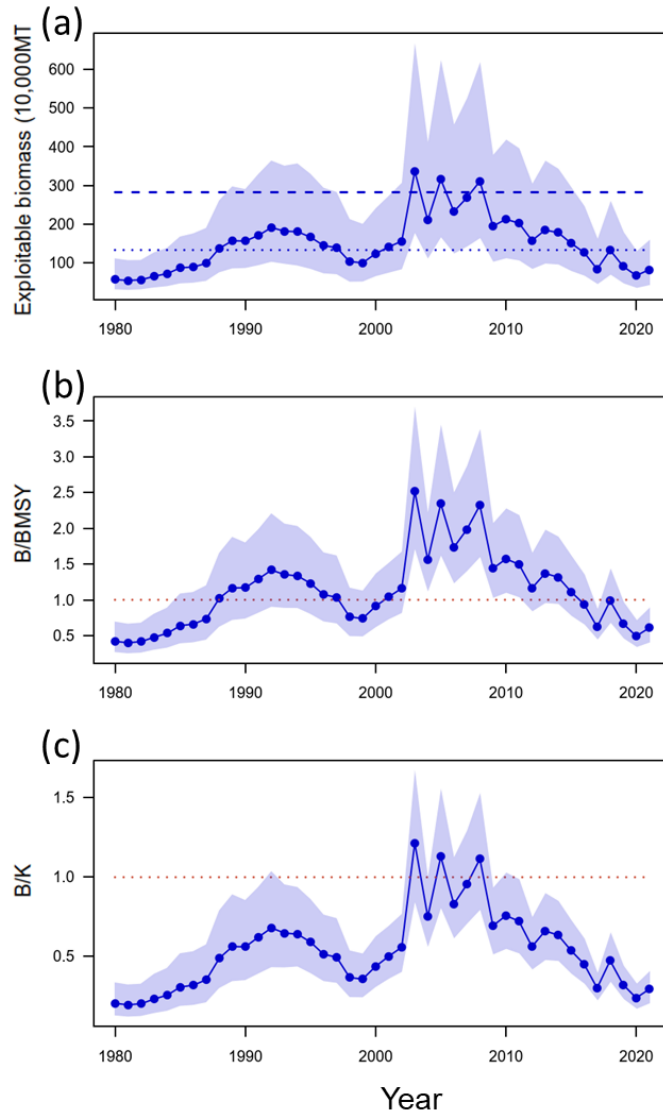


Figure S1. Time series of biomass (10,000 metric ton) (a), ratio of biomass to  $B_{MSY}$  ( $B/B_{MSY}$ ) (b), and depletion ratio ( $B/K$ ) of the western North Pacific saury for the base case 1. In panel (a), the upper dashed and lower dotted horizontal line denotes the carrying capacity ( $K$ ) and  $B_{MSY}$ , respectively. In panels (b) and (c), the dashed lines denote the reference levels of 1.

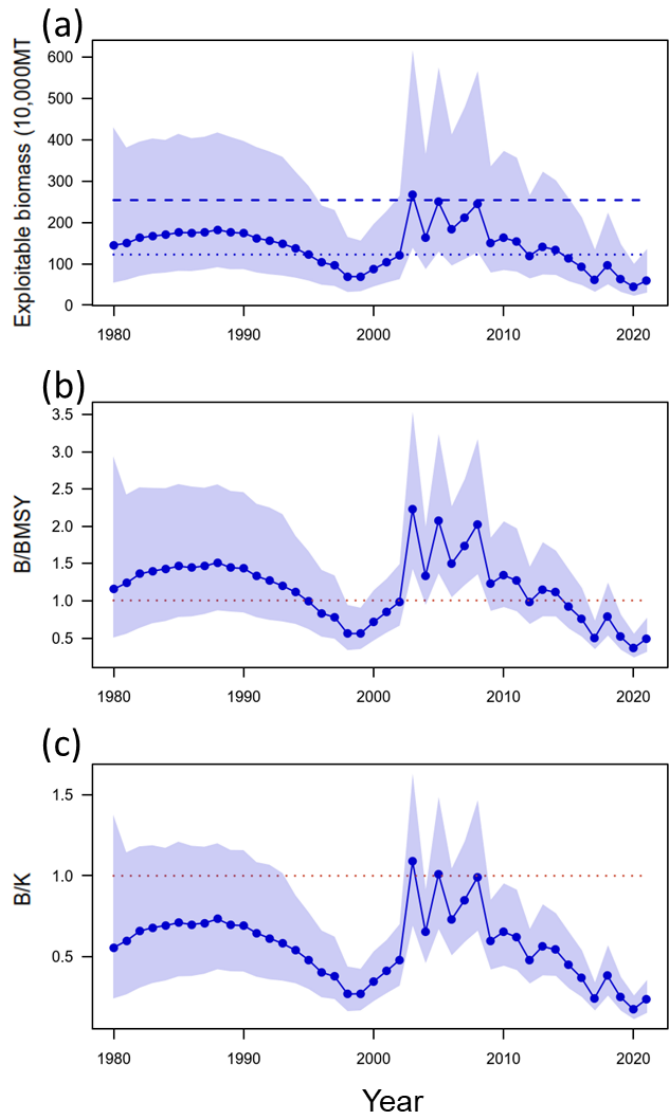


Figure S2. Time series of biomass (10,000 metric ton) (a), ratio of biomass to  $B_{MSY}$  ( $B/B_{MSY}$ ) (b), and depletion ratio ( $B/K$ ) of the western North Pacific saury for the base case 2. In panel (a), the upper dashed and lower dotted horizontal line denotes the carrying capacity ( $K$ ) and  $B_{MSY}$ , respectively. In panels (b) and (c), the dashed lines denote the reference levels of 1.

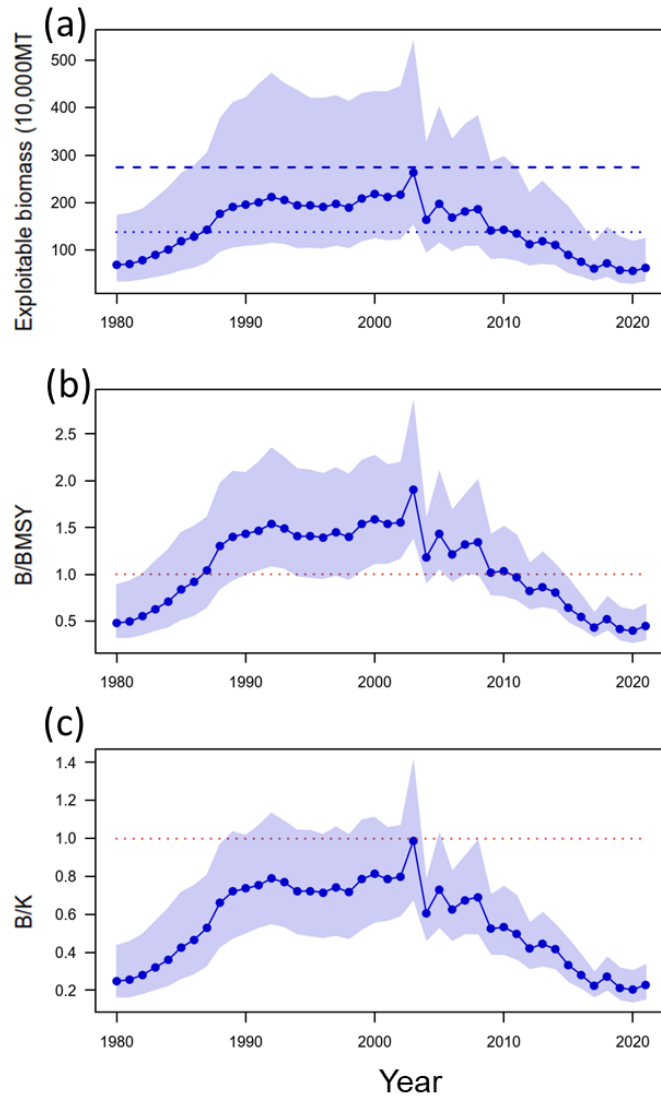


Figure S3. Time series of biomass (10,000 metric ton) (a), ratio of biomass to  $B_{MSY}$  ( $B/B_{MSY}$ ) (b), and depletion ratio ( $B/K$ ) of the western North Pacific saury for the sensitivity case 1. In panel (a), the upper dashed and lower dotted horizontal line denotes the carrying capacity ( $K$ ) and  $B_{MSY}$ , respectively. In panels (b) and (c), the dashed lines denote the reference levels of 1.

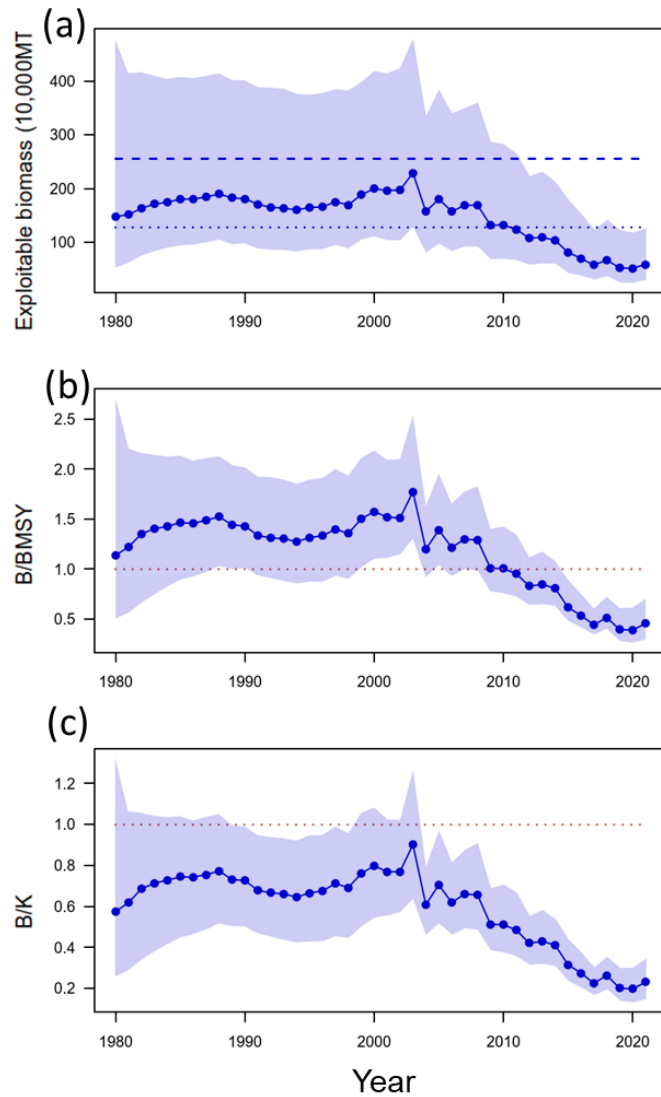


Figure S4. Time series of biomass (10,000 metric ton) (a), ratio of biomass to  $B_{MSY}$  ( $B/B_{MSY}$ ) (b), and depletion ratio ( $B/K$ ) of the Western North Pacific saury for the sensitivity case 2. In panel (a), the upper dashed and lower dotted horizontal line denotes the carrying capacity ( $K$ ) and  $B_{MSY}$ , respectively. In panels (b) and (c), the dashed lines denote the reference levels of 1.

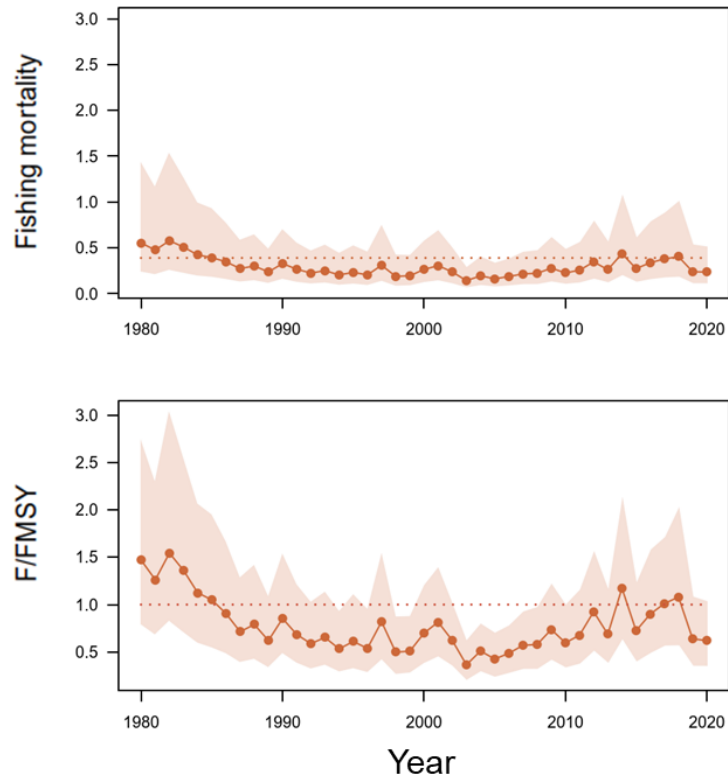


Figure S5. Time series of fishing mortality (a) and ratio of fishing mortality to  $F_{MSY}$  ( $F/F_{MSY}$ ) (b) of the Western North Pacific saury for the base case 1. In panel (a), the dashed line denotes the  $F_{MSY}$ . In panels (b), the dashed line denotes the reference levels of 1.

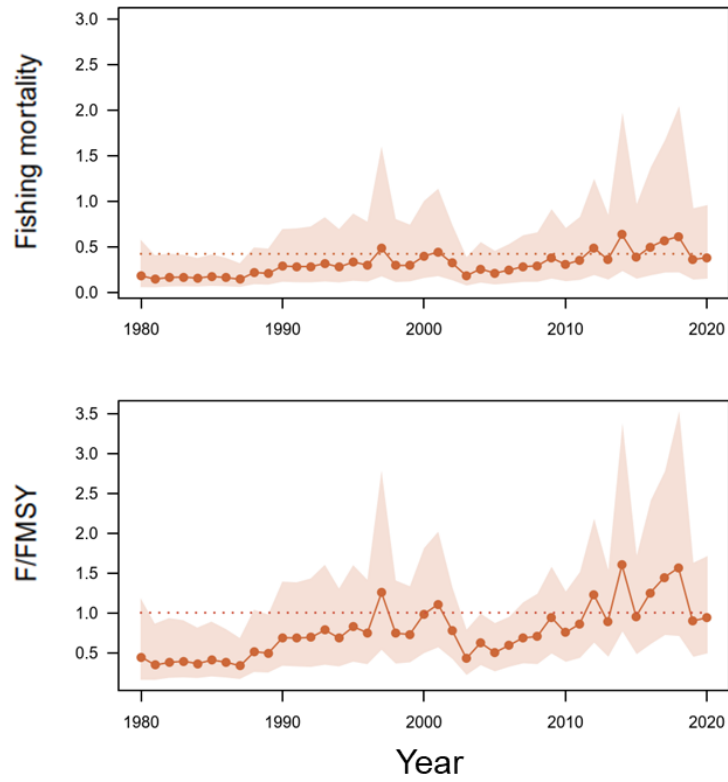


Figure S6. Time series of fishing mortality (a) and ratio of fishing mortality to  $F_{MSY}$  ( $F/F_{MSY}$ ) (b) of the Western North Pacific saury for the base case 2. In panel (a), the dashed line denotes the  $F_{MSY}$ . In panels (b), the dashed line denotes the reference levels of 1.

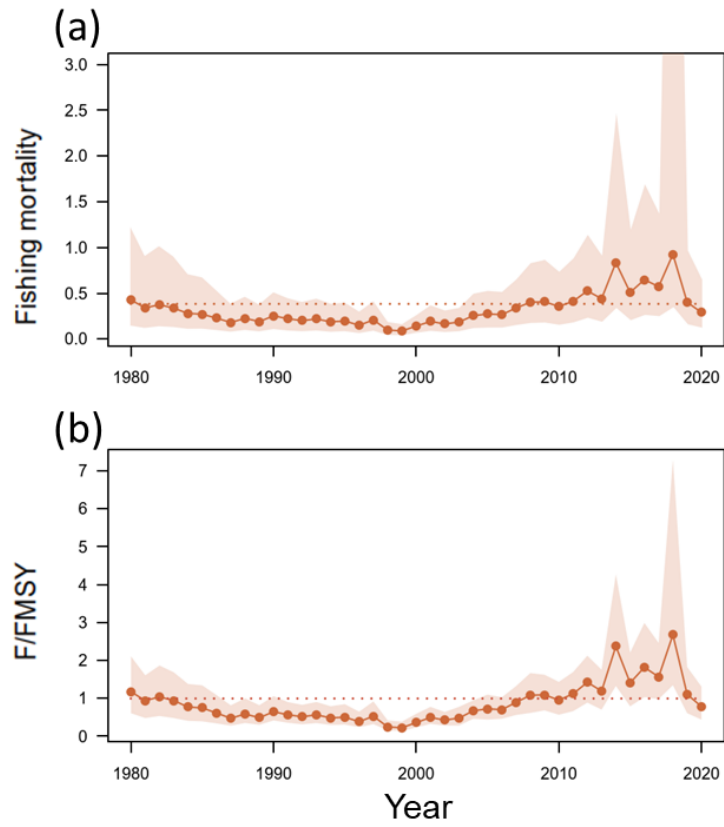


Figure S7. Time series of fishing mortality (a) and ratio of fishing mortality to  $F_{MSY}$  ( $F/F_{MSY}$ ) (b) of the Western North Pacific saury for the sensitivity case 1. In panel (a), the dashed line denotes the  $F_{MSY}$ . In panels (b), the dashed line denotes the reference levels of 1.

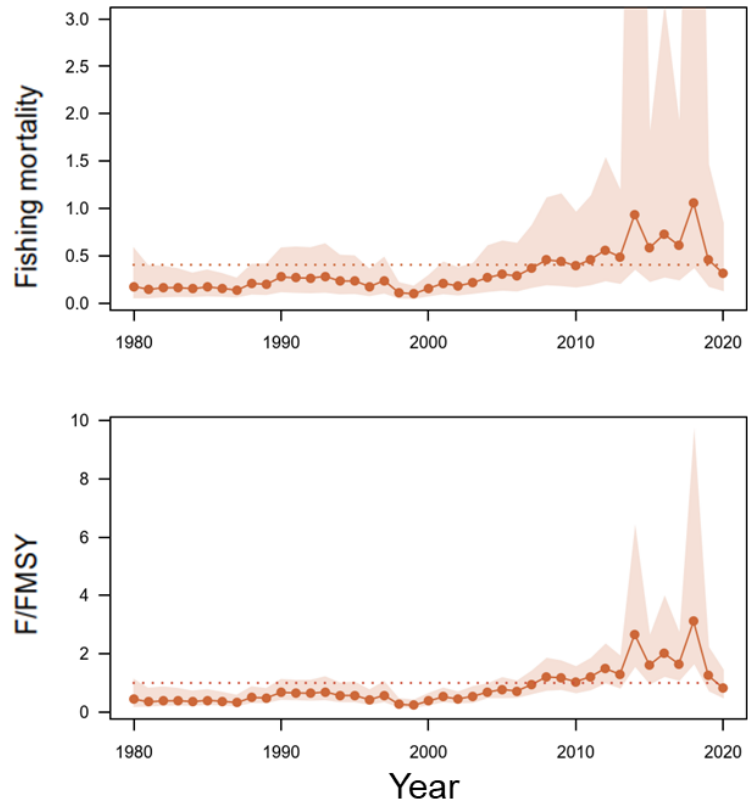


Figure S8. Time series of fishing mortality (a) and ratio of fishing mortality to  $F_{MSY}$  ( $F/F_{MSY}$ ) (b) of the Western North Pacific saury for the sensitivity case 2. In panel (a), the dashed line denotes the  $F_{MSY}$ . In panels (b), the dashed line denotes the reference levels of 1.

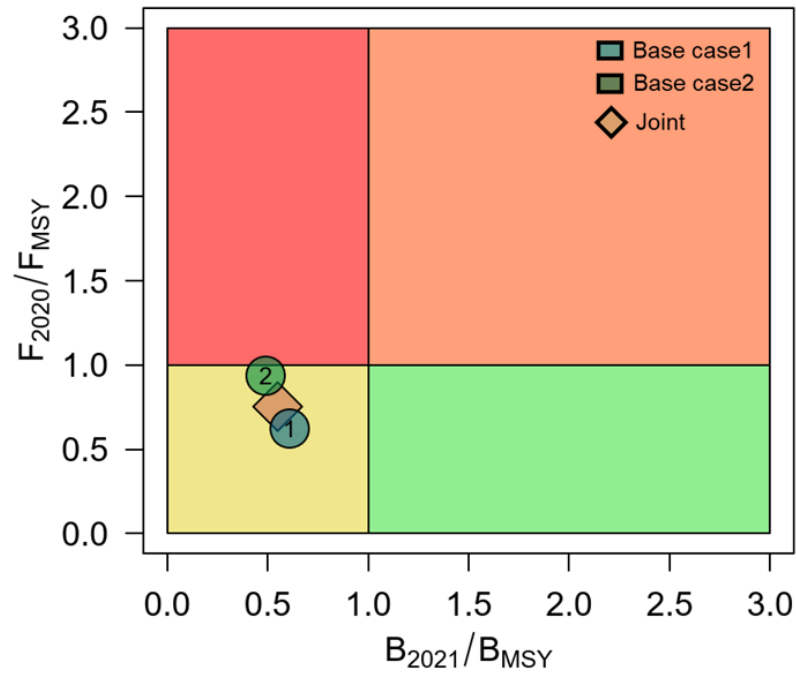


Figure S9. Kobe phase plot of stock status in the last year of Pacific saury from the two base case models. The orange diamond is the median estimate of MCMC results from the two base case models.

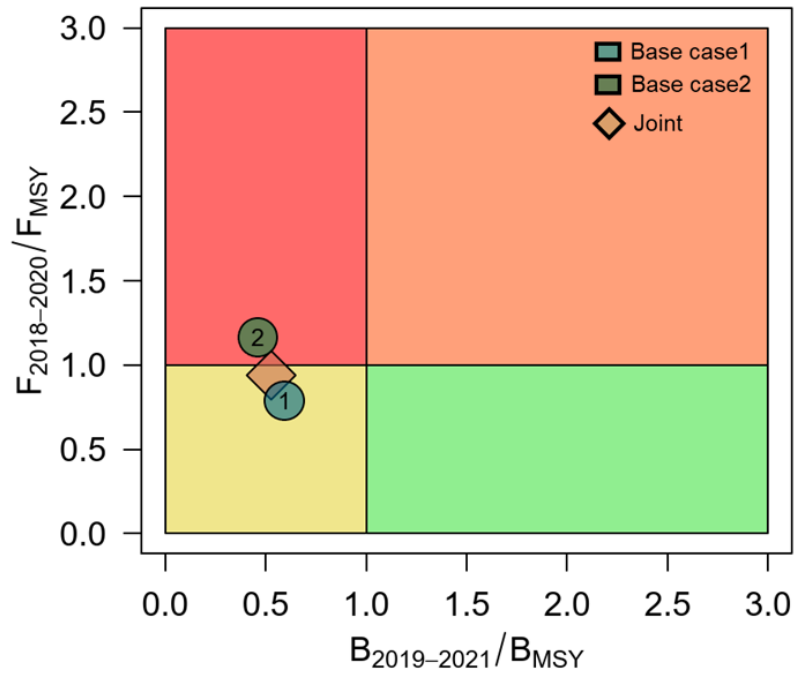


Figure S10. Kobe phase plot of average stock status ( $B_{2019-2021}/B_{MSY}$  and  $F_{2018-2020}/F_{MSY}$ ) of Pacific saury from the two base case models. The orange diamond is the median estimate of MCMC results from the two base case models.